Variation in P-O Bonding in Phosphate Glasses – A Neutron Diffraction Study

Uwe Hoppe, Rainer Kranold, Dörte Stachel[a], Andrea Barz[a], and Alex C. Hannon[b]

Universität Rostock, Fachbereich Physik, D-18051 Rostock
[a] Friedrich-Schiller-Universität Jena, Otto-Schott-Institut, Chemisch-Geowissenschaftliche Fakultät, D-07743 Jena
[b] ISIS Facility, Rutherford Appleton Laboratory, Chilton, Didcot OX11 0QX, UK

Reprint requests to Dr. U. H.; Fax: + 49 381 4981726, E-mail: Hoppe@physik1.uni-rostock.de

Z. Naturforsch. **55 a,** 369–380 (2000); received October 6, 1998

Two different lengths of P-O bonds in the PO_4 units of phosphate glasses are found by neutron diffraction experiments of high resolution in real space. The two lengths are related to bonds of the phosphorus atom with the terminal and the bridging oxygen atoms. The mean lengths and widths of both P-O distance peaks change as a function of the glass composition. In a large range, starting from vitreous P_2O_5 up to the pyrophosphate composition, the behavior of the bond lengths is compared with that in the related crystals and with that resulting from ab initio calculations. The bond lengths depend not only on the species of the participating oxygen atoms and on the number of links of the concerning PO_4 unit but also on the number of links of the neighboring PO_4 unit and on the species of the modifier cation.

Key words: Neutron Diffraction; Short-range Order; Phosphate Glasses.

1. Introduction

PO_4 tetrahedra are the basic structural units of the networks of phosphate glasses. Scattering measurements of high resolution power in real space such as diffraction experiments performed at neutron spallation sources with $Q_{max} \cong 500\ nm^{-1}$ allow to study the detailed lengths of the different P-O bonds within the PO_4 groups [1]. Q is the magnitude of the scattering vector with $Q = 4\pi/\lambda \sin\theta$, where λ is the radiation wavelength and 2θ is the scattering angle. The distance peak of the P-O bond is split into two contributions. This behavior is observed in all diffraction studies which make use of that high resolution power mentioned above [1 - 6]. Previously, we reported some comparisons of the parameters of the distance peaks, i. e. their areas, positions and widths, of a small series of metaphosphate glasses with different modifier cations [3] and of a compositional series of ultraphosphate glasses [4]. The recent measurements of some more samples [5, 6, this work] extend the compositional range available for discussion of the character of the P-O bonds. A thorough analysis of the bonds in phosphate glasses becomes possible starting from vitreous P_2O_5 [5] up to the pyrophosphate composition. Before the concerning discussion starts, the knowledge about the way of linking between the PO_4 units is resumed briefly.

The structural behavior listed below is reviewed in [7] and has been examined numerously by O1s X-ray photoelectron spectroscopy (XPS) [8 - 11], ^{31}P magic angle spinning (MAS) NMR [11 - 14] and vibrational spectroscopy (Raman scattering, Infrared absorption) [11, 14 - 20]. Four of the five valence electrons of the phosphorus atom form an sp^3 hybrid orbital which implies tetrahedral geometry of the oxygen atoms surrounding the phosphorus atom. The fifth electron, populating a d-orbital, joins in a π-bond with one of the oxygen atoms, making this a doubly bonded and a terminal site (O_T). Thus, the network structure of pure P_2O_5 glass is formed of corner-linked tetrahedral units but equipped with already 40% of the oxygen atoms on unlinked corners. The addition of modifier oxide leads to the rupture of P-O-P bridges altering bridging oxygens (O_B) into further O_T atoms. In a common terminology of nuclear magnetic resonance (NMR) spectroscopy, Q^n denotes a PO_4 tetrahedron with n being the number of its links with other PO_4

0932–0784 / 00 / 0300–0369 $ 06.00

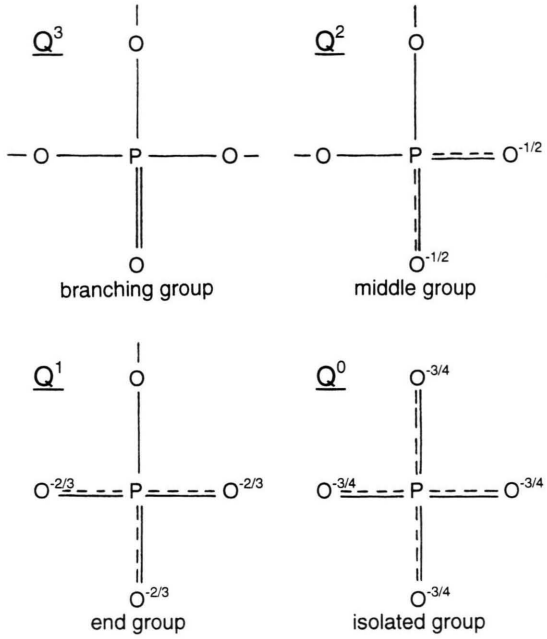

Fig. 1. The four possible Q^n units in phosphate glasses (n: number of links). According to the delocalization of π-bonding, the double bond and the electron charge are split on all the terminal oxygen sites of a given PO_4 group.

units. The four possible Q^n units are illustrated in Figure 1. In the Q^n unit of a given n, the P-O_T bonds cannot be differentiated according to their origin either being formed in the branching unit or caused by the network rupture. The π-bond character and the negative charge depleted from the modifier atom are delocalized on all the O_T sites of a given Q^n group.

As predicted by Van Wazer [21] and as confirmed by ^{31}P MAS NMR [11 - 14], in a phosphate glass of a given modifier content the fractions of the various Q^n units do not obey a random rule but appear in binary distributions. Starting from vitreous P_2O_5 formed of Q^3 units, only two types, Q^3 and Q^2 groups, co-exist in glasses of the ultraphosphate range ($0 < y < 1$). As a measure of the modifier content, the ratio $y = n(Me_{2/v}O)/n(P_2O_5)$ is introduced, where v is the valency of the modifier atom Me. In the ultraphosphate range the fraction of the Q^2 units, f_2, is equal to y. Note, f_2 would be equal to $x/(1 - x)$ when the mole fraction, x, of the modifier oxide is used [11]. At metaphosphate composition ($y = 1$) the glasses are formed of infinite chains and/or rings of twofold linked PO_4 units (Q^2). Further addition of modifier oxide leads to a rupture of the chains which are terminated by Q^1 units. Assuming that in the polyphosphate range ($1 < y < 2$) Q^0 units do not occur, the fraction of Q^1, f_1, is equal to $y - 1$ [14]. According to this scheme, at the pyrophosphate composition ($y = 2$) only Q^1 units are expected. Actually, in the vicinity of this glass composition a weak disproportionation reaction of Q^1 groups into Q^0 and Q^2 units is detected [14, 22]. The mean numbers of the P-O_T and P-O_B bonds per P atom are independent of this reaction. They change continuously with $N_{POT} = y$ and $N_{POB} = 3 - y$, respectively [7, 8]. These numbers can be correlated with the areas of the P-O_T and P-O_B distance peaks which are obtained by the diffraction experiments [1 - 6]. But in this work it is rather planned to study the detailed behavior of the lengths of the P-O_T and P-O_B bonds in the various Q^n groups as functions of the composition y and of the species of modifier cation.

Previously, we discussed the changes of the P-O_T and P-O_B distances in the range of ultraphosphate glasses [4]. It is known that the two bond lengths of the Q^3 unit of vitreous P_2O_5 [5] are different from the corresponding lengths of the Q^2 unit of a metaphosphate glass [3]. But in the ultraphosphate range where a mixture of Q^3 and Q^2 units exists, only two instead of four different P-O distances are detectable [4]. In order to resolve more details than only the two P-O distances already obtained in the ultraphosphate structures, two sodium phosphate glasses, a metaphosphate glass with $y = 1$ and an ultraphosphate glass with $y = 0.6$, have been chosen for the present study. In case of alkali modified glasses only a small effect of disorder on the geometry of the PO_4 units is caused by the modifier cations [3]. Moreover, at $y = 0.6$ a maximum number of links between unlike units, Q^3 and Q^2, can be formed [4] while in vitreous P_2O_5 such as in $NaPO_3$ only one species of Q^n units exists, either Q^3 or Q^2 [11], and thus, only links between equal groups are formed.

As a second point of investigation, a small number of samples beyond the metaphosphate composition is studied. Diffraction experiments of high resolution power in real space of such glasses have not been made before. Some further metaphosphate samples have been measured to study the structural effects of ternary glasses. In this work only the information about their P-O distances is extracted. The other results, such as the changes of the oxygen environments of the modifier cations in the sodium, the lead and the ternary phosphate glasses, will be presented in subsequent papers together with the corresponding X-ray

Table 1. Mass densities and parameters of the preparation of the samples studied. The sodium ultraphosphate glass was prepared in a sealed silica ampule.

Sample composition	Density [g/cm^3]	Crucible	Melting time [h]	Temperature [°C]
$(Na_2O)_{0.379}$-$(P_2O_5)_{0.621}$	2.440	ampoule	0.5	900
$(Na_2O)_{0.50}$-$(P_2O_5)_{0.50}$*	2.50	SiO_2	0.5	900
$(PbO)_{0.61}$-$(P_2O_5)_{0.39}$	5.702	SiO_2	0.5	1000
$(ZnO)_{0.107}$-$(PbO)_{0.505}$-$(P_2O_5)_{0.388}$	5.245	SiO_2	0.5	1000
$(ZnO)_{0.102}$-$(PbO)_{0.558}$-$(P_2O_5)_{0.34}$	5.825	SiO_2	0.5	1000
$(ZnO)_{0.10}$-$(PbO)_{0.40}$-$(P_2O_5)_{0.50}$*	4.28	SiO_2	1.0	900
$(ZnO)_{0.102}$-$(CaO)_{0.353}$-$(P_2O_5)_{0.545}$	2.68	SiO_2	1.0	1160
$(ZnO)_{0.087}$-$(SrO)_{0.430}$-$(P_2O_5)_{0.483}$	3.18	SiO_2	1.0	1280

* For the sodium and the Zn/Pb metaphosphate glasses the nominal composition of the batch are used.

diffraction data. The analysis of the P-O peaks of the glasses is accompanied by comparisons with the parameters of related crystal structures [23 - 36].

2. Experimental

2.1. Sample Preparation

The mass densities, compositions and parameters of the sample preparation are given in Table 1. The mass densities were obtained by the Archimedes method. The compositions of the upper samples were determined by wet chemical methods. The compositions of the lower two samples result from electron scanning micro analysis (ESMA). The glass samples containing 10 mol% ZnO are adopted to this paper only according to their use in the discussion of the P-O distances. Specifics of the Zn-O and Pb-O environments as well as information about the medium-range order will be presented in subsequent papers.

2.2. Diffraction Experiments

The neutron diffraction experiments were performed on the liquids and amorphous's diffractometer (LAD) at the ISIS facility of the Rutherford Appleton Laboratory, England. For the measurements, crushed pieces of the glasses were filled into vanadium containers of 11 mm diameter. During the data collection, using time-of-flight technique, the container was located in a vacuum chamber. In case of the two sodium phosphate glasses the sample runs took 20 hours. About 12 hours were used for every of the other sample runs. The incident neutron spectrum was obtained by use of a vanadium rod of 8 mm in diameter. The raw data were corrected by standard procedures for attenuation, multiple scattering, inelasticity effects, and for container and background scattering using the program suite ATLAS [37] which is available at ISIS. Finally, all that results in the normalized differential scattering cross-sections, $d\sigma/d\Omega$. The data have been converted into the static structure factors, $S(Q)$, by

$$S(Q) = \{d\sigma/d\Omega - [\langle b^2\rangle - \langle b\rangle^2]\}/\langle b\rangle^2, \quad (1)$$

where b_i is the neutron scattering length of atoms of sort i and $\langle ...\rangle$ means the average in respect of the sample composition. $\langle b^2\rangle$ includes also the incoherent scattering in respect of the various spin and isotopic contributions.

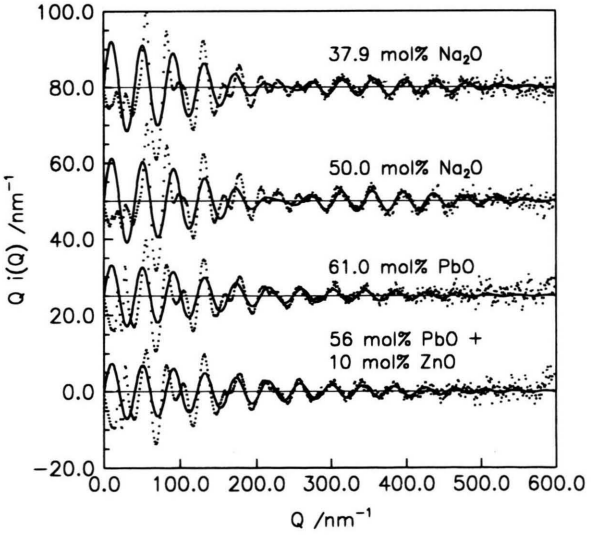

Fig. 2. Weighted interference functions of four of the phosphate glasses studied (experimental data: dots). The content of modifier oxide is indicated in the plot. For comparison, the model functions calculated by the parameters of two Gaussian functions (cf. Table 2) used to approximate the distances peaks of the P-O bonds are drawn as solid lines.

Table 2. Parameters of the fit of the distance peaks of the P-O_T and the P-O_B neighbors, total P-O coordination numbers and mean distances. The distances and the fwhm are given in pm.

Atom pair	Coordin. number	Distance	fwhm fwhm	Total coordination no.	Mean distance
$(Na_2O)_{0.379}$-$(P_2O_5)_{0.621}$					
P-O_T	1.59(8)	146.8(8)	9.5(8)	3.96(20)	154.8(8)
P-O_B	2.37(12)	160.2(8)	12.5(10)		
$(Na_2O)_{0.50}$-$(P_2O_5)_{0.50}$					
P-O_T	2.00(10)	147.8(8)	9.6(8)	4.00(20)	154.6(8)
P-O_B	2.00(10)	161.4(8)	10.5(10)		
$(PbO)_{0.50}$-$(P_2O_5)_{0.50}$ [2]					
P-O_T	1.92(10)	148.5(10)	10.0(10)	3.85(20)	154.4(8)
P-O_B	1.93(10)	160.3(10)	11.7(10)		
$(PbO)_{0.61}$-$(P_2O_5)_{0.39}$					
P-O_T	2.69(12)	151.1(10)	10.7(8)	4.19(20)	155.6(8)
P-O_B	1.50(8)	163.6(10)	13.4(10)		
$(ZnO)_{0.107}$-$(PbO)_{0.505}$-$(P_2O_5)_{0.388}$					
P-O_T	2.58(12)	150.9(10)	10.7(8)	4.13(20)	155.3(8)
P-O_B	1.55(8)	162.6(10)	13.3(10)		
$(ZnO)_{0.102}$-$(PbO)_{0.558}$-$(P_2O_5)_{0.34}$					
P-O_T	2.98(12)	152.1(8)	10.4(8)	4.05(20)	155.3(8)
P-O_B	1.07(8)	164.3(10)	12.1(10)		
$(ZnO)_{0.10}$-$(PbO)_{0.40}$-$(P_2O_5)_{0.50}$					
P-O_T	1.88(10)	148.7(8)	10.4(10)	3.76(20)	154.6(8)
P-O_B	1.88(10)	160.6(10)	11.4(10)		
$(ZnO)_{0.102}$-$(CaO)_{0.353}$-$(P_2O_5)_{0.545}$					
P-O_T	1.83(10)	148.1(8)	9.7(8)	3.81(20)	154.4(8)
P-O_B	1.98(10)	160.3(10)	11.0(10)		
$(ZnO)_{0.087}$-$(SrO)_{0.430}$-$(P_2O_5)_{0.483}$					
P-O_T	2.02	148.5	9.6(8)	3.95(20)	154.7(8)
P-O_B	1.93	161.1	10.8(10)		

3. Results

For illustration of the accuracy of the scattering data the weighted interference functions, $Q \cdot i(Q)$, with $i(Q) = S(Q) - 1$, of the sodium and lead phosphate glasses are shown in Figure 2. Model functions were calculated for comparison according to (1) of [5], using the parameters of the two Gaussian functions which fit the two P-O distance peaks (see below). For $Q > 300\ \mathrm{nm}^{-1}$, only information about these distances is relevant. In general, the noise of the experimental data limits their use for $Q > 500\ \mathrm{nm}^{-1}$. This limit is chosen as the Q_{max} in the Fourier integral (2). Information about the lengths of the P-O bonds has been extracted by modelling the first distance peak positioned at about 155 pm in the real-space correlation

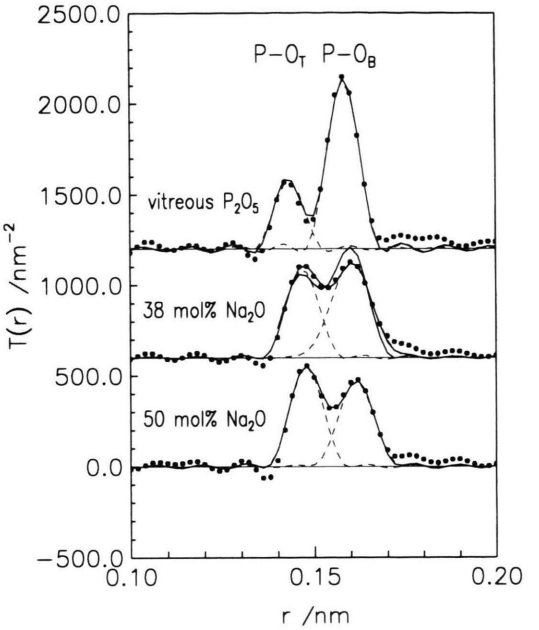

Fig. 3. P-O peaks in the real-space correlation function, $T(r)$, of vitreous P_2O_5 [5] and of two sodium phosphate glasses. Experimental data: dotted lines, total fit: solid lines, P-O_T and P-O_B bonds: dashed lines. The solid-lined function which does not fit the data of the glass with 38 mol% Na_2O is explained in the text.

function, $T(r)$. This function results from the $S(Q)$ data by

$$T(r) = 4\pi r \rho_0 + \frac{2}{\pi} \int_0^{Q_{max}} [S(Q) - 1] \sin(Qr) Q \, \mathrm{d}\, Q. \quad (2)$$

ρ_0 is the number density of atoms. The termination effect of the Fourier transformation is taken into account by folding the model peaks with appropriate peak functions [38]. The full width at half maximum (fwhm) of this peak is equal to 7.6 pm for $Q_{max} = 500\ \mathrm{nm}^{-1}$ [39]. The termination effect causes a broadening of the distance peaks and the occurrence of some satellite ripples. No modification function for their damping was applied.

Two Gaussian functions, each of both determined by coordination number, mean position and fwhm, have been used in the least-squares fits [40] of the P-O bond distances in the $T(r)$ data. The fwhm parameters obtained in this way are independent of the Q_{max}. Since in some cases a fit using the corresponding six parameters did not result in the expected ratio of N_{POT} and N_{POB}, at last, this ratio was fixed. This

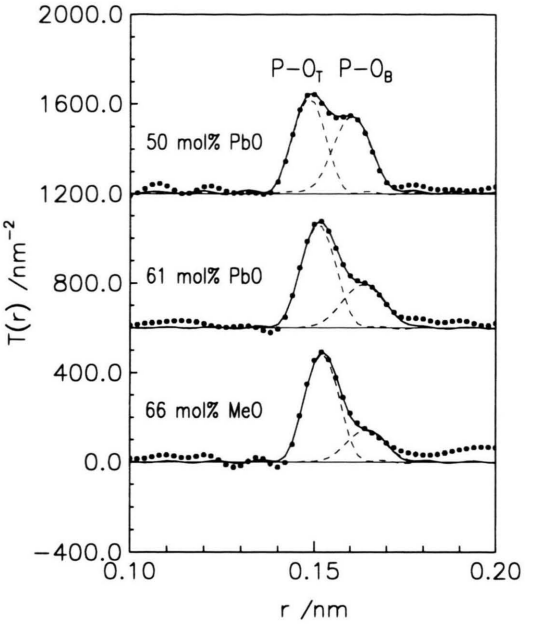

Fig. 4. P-O peaks in the real-space correlation function, $T(r)$, of lead phosphate glasses. Experimental data: dotted lines, total fit: solid lines, P-O_T and P-O_B bonds: dashed lines. MeO stands for a glass with 56 mol% PbO and 10 mol% ZnO. The data of the PbO-P_2O_5 glass are taken from [2].

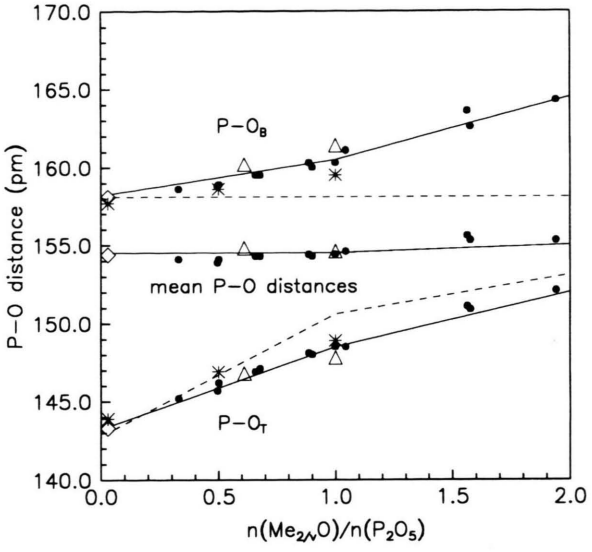

Fig. 5. Compositional behavior of the lengths of the two P-O bonds. Vitreous P_2O_5 [5]: rhombes, modified phosphate glasses with Me = Zn, Ca, Pb [2,4, this work]: filled circles, Na phosphate glasses: triangles. The asterisks denote results from ab initio MO calculations [41]. The solid lines are guides to the eye. The dashed lines give the behavior according to a model of bond order (cf. text), where the P-O_T and P-O_B distances of vitreous P_2O_5 [5] are used as the lengths of the real terminal P=O double bond and the P-O_B single bond.

constraint causes no significant changes of the distances and fwhm of the other samples. The resulting parameters of the P-O distances of the glasses of the present study are given in Table 2. The determination of all the parameters of the previous measurements [2 - 6], which also will be used in the subsequent comparisons, have been repeated under the same conditions as described above. Figure 3 shows the peaks of the P-O distances of the two sodium phosphate glasses studied in comparison with those of vitreous P_2O_5. The P-O peaks of three lead phosphate glasses, starting with the metaphosphate glass and up to the pyrophosphate composition are compared in Figure 4.

4. Discussion

4.1. The Compositional Dependencies of the Lengths of the Two P-O Bonds

In the search for more details than only the existence of two P-O bonds, a sodium ultraphosphate glass of 37.9 mol% Na_2O was chosen for the measurements. However, no new details of the P-O_T and P-O_B distance peaks became obvious. The behavior of the widths of the P-O distance peaks observed is discussed in the subsequent chapter.

An analysis of the behavior of the lengths of the different P-O bonds in the PO_4 units was already presented for a series of ultraphosphate glasses [4, 5]. The behavior of the bond lengths in the more extended compositional range now available is shown in Figure 5. New data are presented for two sodium phosphate glasses (triangles) and for several meta- and polyphosphate glasses ($y \geq 1$). The P-O distances of ab initio molecular orbital (MO) calculations [41] are shown as asterisks. For vitreous P_2O_5 these lengths agree with the experimental data [5]. The other MO data follow the trends of the experimental results.

The strongest obvious effect is an increase of the lengths of the P-O_T bonds. Roughly, this behavior can be approximated by taking into account a decrease of their bond order. In a simple model one can assume the bond order of the P=O double bond being two and the bond order of the P-O_B bond being one.

Table 3. Mean lengths of the P-O bond, the $P\text{-}O_T$ and $P\text{-}O_B$ distances and the molar ratio, y, with $y = n(Me_{2/\nu}O) / n(P_2O_5)$, of selected phosphate crystals, where ν is the valency of Me. The distances are given in pm.

Crystalline compound	y	P-O	$P\text{-}O_T$	$P\text{-}O_B$	Ref.
o-P_2O_5 (form II)	0.0	154.3	144.5	157.6	[23]
ZnP_4O_{11}	0.5	153.6	145.7	158.3	[24]
NdP_5O_{14}	0.6	153.8	146.7	158.5	[25]
$Ca_2P_6O_{17}$	0.66	153.7	147.2	158.4	[26]
AlP_3O_9	1.0	153.0	148.3	157.7	[27]
LaP_3O_9	1.0	153.5	148.3	158.7	[28]
$NaPO_3$ Kurrol A	1.0	154.4	147.8	161.0	[29]
KPO_3	1.0	154.8	146.8	162.8	[30]
$Mg_2Na_2P_5O_{16}$	1.4	153.9	149.8	160.1	[31]
$Pb_3P_4O_{13}$	1.5	154.1	150.7	159.7	[32]
$Na_5P_3O_{10}$	1.66	154.6	150.0	163.8	[33]
$Na_4P_2O_7$	2.0	154.4	151.3	163.6	[34]
$Pb_2P_2O_7$	2.0	153.8	151.1	162.0	[35]
Na_3PO_4	3.0	154.7	154.7	–	[36]

The corresponding lengths are taken from the P-O bonds of the Q^3 units of vitreous P_2O_5 (143.2 pm and 158.1 pm) [5]. The bond orders of the $P\text{-}O_T$ bonds in the Q^2, Q^1, and Q^0 units are 1.5, 1.33, and 1.25, respectively [11]. The lengths of the bonds are assumed to increase according to their decrease of bond order. They are calculated taking into account the fractions of the Q^n (cf. Introduction). The $P\text{-}O_T$ and $P\text{-}O_B$ lengths should behave as predicted by the dashed-lined functions shown in Figure 5. Actually, such as predicted by the bond order model, the mean P-O distances do not change as a function of the glass composition. But the real $P\text{-}O_T$ bonds are slightly shorter than predicted, and the $P\text{-}O_B$ bonds measured increase, though they should be constant. In the limit of Q^0 groups with a bond order of 1.25 ($y = 3.0$) the $P\text{-}O_T$ lengths seem to approach the predicted length of 154.4 pm. Actually, a length of 153.6 pm was reported for a $P_{0.5}V_{1.5}O_5$ glass [42] where only Q^0 units exist.

Also the MO results [41] deviate from the behavior predicted by the bond order model except of the $P\text{-}O_T$ length of the cluster with $y = 0.5$. In [4] we attributed these slight deviations from our experimental data to deficits in the environment of the O_T atom of the Q^3 unit of the $H_3NaP_2O_7$ cluster used in the MO calculations [41]. The behavior of the P-O distances found in selected crystalline phosphates (cf. Table 3) complies with the tendencies indicated by the experimental data of all the phosphate glasses studied.

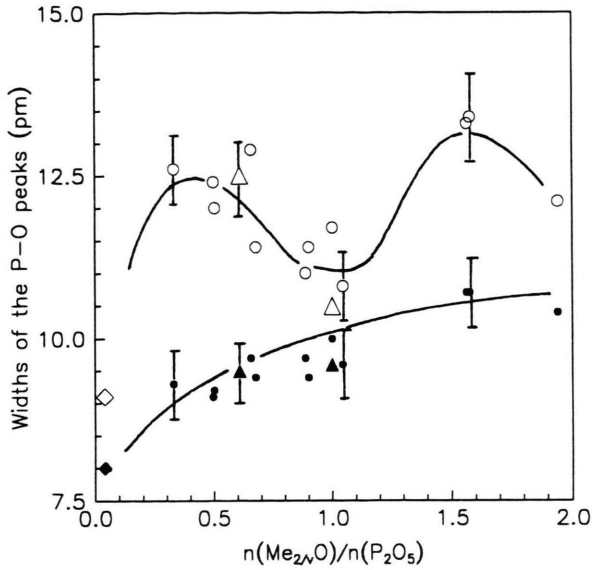

Fig. 6. Compositional behavior of the widths of the two P-O distance peaks. Vitreous P_2O_5 [5]: rhombes, modified phosphate glasses with Me = Zn, Ca, Pb [2, 4, this work]: circles, sodium phosphate glasses: triangles. The filled symbols denote the fwhm of the $P\text{-}O_T$ bond, hollow symbols are the data of the $P\text{-}O_B$ bond. The lines are guides to the eye.

4.2. *The Compositional Dependencies of the Widths of the Two P-O Distance Peaks*

Other parameters of the two P-O distance peaks, such as their widths, may also be examined in analysing the behavior of the bond lengths in phosphate glasses. These parameters cannot be related with equivalent data of crystal structures. The behavior of the widths of the $P\text{-}O_T$ and $P\text{-}O_B$ peaks (cf. Fig. 6) may give more insight into details of the bonds between the various P and O sites of different Q^n units. At first, the widths of the $P\text{-}O_T$ peaks (filled symbols) increase weakly but monotonously. On the other hand, the widths of the $P\text{-}O_B$ peaks (hollow symbols) show maxima for those glass compositions where an intense mixing of differently linked PO_4 units exists (Q^3 and Q^2 at $y \cong 0.5$; Q^2 and Q^1 at $y \cong 1.5$). The total changes of the $P\text{-}O_T$ lengths are larger than the changes of the $P\text{-}O_B$ lengths, but the widths of the $P\text{-}O_T$ peaks are smaller than those of the $P\text{-}O_B$ peaks. Thus, the $P\text{-}O_T$ and $P\text{-}O_B$ lengths found for the ultraphosphate glasses are not the means of a distribution of lengths of unlike Q^n groups with different but rigid bonds. Obviously, the lengths of the P-O bonds of a given Q^n unit are affected by the environment, e. g.,

Table 4. Comparison of the mean lengths of the P-O bond in different structural positions of those phosphate crystals which are already used in Table 3. The bonds are classified according to their participation in the different Q^n units. Additionally, the P-O_B bonds are differentiated according to their positions in links with different Q^n units. The distances are given in pm.

Crystalline compound	— P-O_T —			— P-O_B in Q^3 —		— P-O_B in Q^2 —			— P-O_B in Q^1 —	
	Q^3	Q^2	Q^1	$\Rightarrow Q^3$	$\Rightarrow Q^2$	$\Rightarrow Q^3$	$\Rightarrow Q^2$	$\Rightarrow Q^1$	$\Rightarrow Q^2$	$\Rightarrow Q^1$
o-P_2O_5 (form II)	144.5	–	–	157.6	–	–	–	–	–	–
ZnP_4O_{11}	145	146	–	157	155.5	162	–	–	–	–
NdP_5O_{14}	146	147	–	–	156	161	–	–	–	–
$Ca_2P_6O_{17}$	146	147.5	–	–	156	161	158	–	–	–
LaP_3O_9	–	148.3	–	–	–	–	158.7	–	–	–
$NaPO_3$ Kurrol A	–	147.8	–	–	–	–	161.0	–	–	–
$Mg_2Na_3P_5O_{16}$	—	149.0	150.6	–	–	–	158.6	157.7	165.6	–
$Pb_3P_4O_{13}$	–	148.6	152.1	–	–	–	159.7	157.2	162.1	–
$Na_5P_3O_{10}$	–	148.9	150.4	–	–	–	–	160.7	166.8	–
$Na_4P_2O_7$	–	–	151.3	–	–	–	–	–	–	163.6
$Pb_2P_2O_7$	–	–	151.1	–	–	–	–	–	–	162.0

they may depend on the species of the adjacent Q^n units.

The widths of the first peak belonging to the P-O_T bonds change only smoothly as a function of composition (cf. Figure 6). They start with a small value of 8 pm for the P-O_T bond of the PO_4 branching units of vitreous P_2O_5. In the other limit, the fwhm of the P-O_T peak of the $P_{0.5}V_{1.5}O_5$ glass formed of isolated PO_4 groups is reported to be 10.8 pm [42], where the affects of the termination of the Fourier integral (2) were also taken into account. Thus, all the widths here given are free of experimental affects. The width of 10.8 pm [42] is of the same magnitude as that of the data we found for the polyphosphate glasses. From the small variation of the widths in the ultraphosphate range it was deduced [4] that all the lengths of P-O_T bonds which originally are different in Q^3 and the Q^2 units, must change as a function of their fractions.

The data of the two sodium phosphate glasses studied are used to examine the behavior of the peak widths. Though the P-O peaks of these sodium glasses do not show any new details in the behavior of the P-O bonds, both peak components are better resolved than those of most other glasses studied before [3, 4]. The modelling of the P-O peaks of the glass of 37.9 mol% Na_2O is repeated using modified constraints. At first, the P-O distance peaks are calculated using the expected fractions of the four different P-O bonds of this glass with two lengths of the Q^3 and two lengths of the Q^2 groups. The corresponding parameters of bond lengths and peak widths are taken from the glasses which are formed of only one species of the participating PO_4 groups, i. e. from vitreous P_2O_5 and from the $NaPO_3$ glass (cf. Table 2). The resulting model function is shown (Fig. 3) as that solid curve which does not fit the experimental $T(r)$ data (points) of the glass with 37.9 mol% Na_2O. The peak of the P-O_T component is too broad while that of the P-O_B component is too narrow.

The parameters used in this model function are the starting parameters for the subsequent fit. The peak areas and widths are fixed but the differences between both P-O_T and between both P-O_B lengths are varied. This fit was successful, and the resulting bond lengths are 145.3 pm (143.3) and 147.3 pm (147.8) for the P-O_T bonds just as 157.0 pm (158.1) and 163.0 pm (161.4) for the P-O_B bonds in the Q^3 and Q^2 units, respectively. The parameters in parentheses are the data taken from vitreous P_2O_5 [5] and from the $NaPO_3$ glass. Thus, the different P-O_T distances of the Q^3 and Q^2 groups tend to equalize. On the other hand, the difference between the P-O_B distances of the Q^3 and Q^2 groups increases.

For simplicity, it was assumed that a single P-O_B distance is typical for a given Q^n unit. As pointed out in [4] this is exact in the case if all the P-O-P bridges are in equal Q^3-Q^2 links such as found, e. g., in the NdP_5O_{14} crystal [25]. Here the P-O_B distances of Q^3 and Q^2 units differ by 5 pm, while the difference between both P-O_T distances is only 1 pm (cf. Table 4). The Na ultraphosphate glass studied has the same molar ratio y as this crystal (37.9 mol% Na_2O). The probability for Q^3-Q^2 linkages is large due to equal total numbers of the P-O_B bonds of both Q^n species. A preference of Q^3-Q^2 links was found by 2D ^{31}P MAS NMR for a glass of similar composition (35 mol%

Na_2O) [43]. By the same method other authors [44] obtained a random formation of the links in Li ultraphosphate glasses. The differences of the two P-O_T and P-O_B distances for the glass of 37.9 mol% Na_2O are 2 pm and 6 pm, respectively. They are very similar with those found in the NdP_5O_{14} crystal [25], though we do not have any knowledge about a preference of Q^3-Q^2 links in the glass.

A similar effect of variations in the peak widths as manifested in the ultraphosphate range is found for the polyphosphate glasses (cf. Fig. 6), though only three of our glass samples exceed the metaphosphate composition. A large width of the P-O_B peak occurs for that glass where the Q^2 and Q^1 units have about equal fractions ($y \approx 1.5$) while the widths of the P-O_T peaks do not vary much.

The effects of the peak widths of the P-O distances shown in Fig. 6 can be resumed as follows: The P-O_T distances tend to equalize not only in a given PO_4 group but also between groups of different numbers of links in case of their co-existence in a common network. A full equalization cannot be concluded from the experimental data. In contrast, the P-O_B distances of unlike PO_4 units, if linked with each other, become more different.

The behavior indicated by the peak widths is compared with that in related phosphate crystals (cf. Table 4). The P-O_T and P-O_B distances which were already given in Table 3 are differentiated according to their location in differently linked PO_4 units. Additionally, the P-O_B bonds are differentiated according to their position in definite Q^n-Q^m linkages. Since some of the glasses studied contain the PbO as the modifier oxide, a few of the selected crystals are Pb phosphates. But due to the huge X-ray scattering power of the Pb atoms the determination of oxygen positions in these crystals is not certain. Therefore, more attention should be paid to the data of the other crystals. On the first glance it becomes obvious that rigid bond lengths do not exist. The P-O_T distances, especially those in the Q^3 and Q^2 units, increase with growing modifier content. The differences between the P-O_T bonds of differently linked PO_4 groups coexisting in the same crystal are less than 2 pm. On the other hand, the main effect of the P-O_B bonds is a strong dependence on their participation in links either with equal Q^n sites or with PO_4 units of a higher or lower number of links. The P-O_B bond of a given Q^n is elongated in case of its use in a link with a Q^{n+1} unit and it is shortened in case of a link with a Q^{n-1} unit. This effect explains the maxima of the widths of the P-O_B peak shown in Figure 6. In [4] the origin of this effect was attributed to an optimization of the charge compensation between the PO_4 units. Before the role of the charge transfer in the bond deformation will be discussed more thoroughly, the smaller but obvious affect of different modifier cations on the P-O bonds is analysed.

4.3. The Dependencies of the P-O Bond Lengths on the Species of the Modifier Cation

As discussed in the previous chapter the main variations of the P-O bonds are due to their function in the phosphate network. Additionally, the bonds are affected by the modifier cations. The data of the metaphosphate glasses are suitable for the analysis of such effects. The P-O peaks in the $T(r)$ functions of five metaphosphate samples which were obtained under like conditions in the experiments and in the data treatment are shown in Figure 7. The $T(r)$ data of three of the glasses have been compared in [3]. A significant change of the lengths and widths is obtained if one compares the effects of cations which

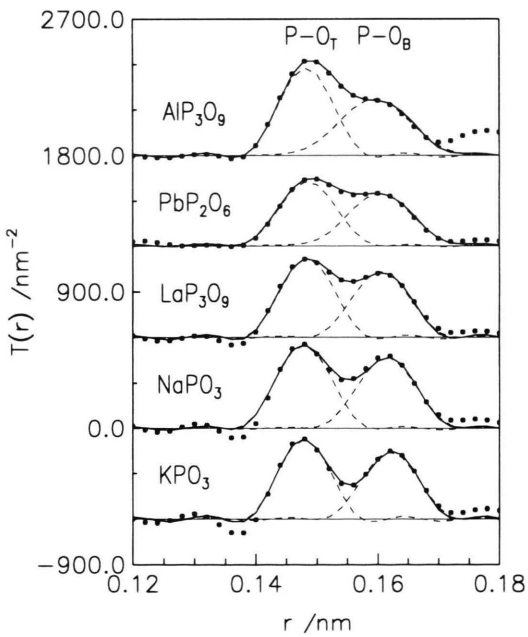

Fig. 7. P-O peaks in the real-space correlation function, $T(r)$, of several metaphosphate glasses (AlP_3O_9, PbP_2O_6 [2]; LaP_3O_9 [6], $NaPO_3$ [this work]; KPO_3 [3]). Experimental data: dotted line, total fit: solid line, P-O_T and P-O_B bonds: dashed line.

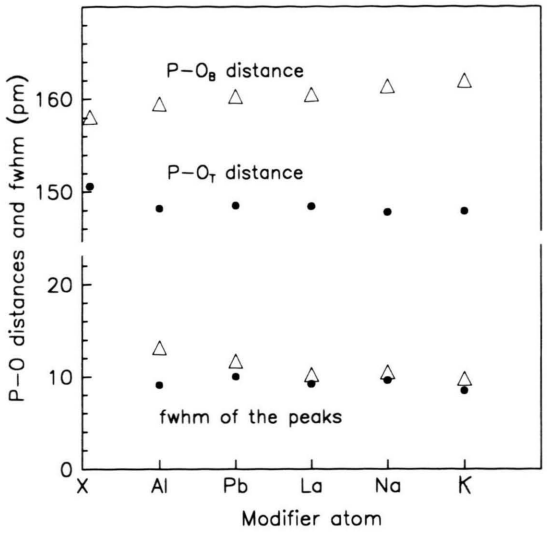

Fig. 8. P-O distances and peak widths (fwhm) corresponding to the P-O peaks shown in Fig. 7 for five metaphosphate glasses. The triangles belong to the P-O_B bond, the points denote data of the P-O_T bond. The points belonging to X on the abscissa correspond to the model of bond order (cf. text) where the P-O distances of vitreous P_2O_5 [5] are used as the unmodified bond lengths.

have different electric field strength. The changes of the lengths and widths of the P-O peaks are shown in Fig. 8 with the data given in the order of the electric field strength of the cations. The P-O bond lengths of a Q^2 unit which are calculated according to the bond order model discussed in Chapt. 4.1 are shown as well, indicated by an X.

The position of the Pb^{2+} cation between Al^{3+} and La^{3+} is chosen according to the extent of the observed changes. Though the La-O distances [6] are slightly shorter than the Pb-O distances [2], and the La^{3+} cation has a higher formal charge one should remember that the oxygen environments of the Pb^{2+}'s in a metaphosphate glass are highly asymmetric due to their two s-electrons [45]. The four or five O_T's at Pb-O distances of $\cong$ 247 pm are affected by a strong charge (Pb^{4+}), while the more distant O_T atoms surrounding the Pb site are allmost not affected [46]. But these O_T atoms are nearest neighbors of other Pb^{2+} sites.

With decreasing electric field strength the P-O_T distances little decrease while the P-O_B distances increase (cf. Figures 7, 8). Thus, the largest mean P-O distance is obtained for the KPO_3 glass. The bond lengths of the related crystals behave similarly (cf. the data given in Table 3). The same findings are known from ab initio MO calculations [47]. Note, the deviations from the bond order model (X in Fig. 8) introduced in Chapt. 4.1 increase with the decreasing electric field strength of the modifier cations. Additionally, the widths of the P-O peaks decrease with decreasing electric field strength of the cations. In glasses whose modifier cations possess only weak ionic forces the geometry of the PO_4 units is more relaxed at the expense of additional disorder in the oxygen polyhedra of the cations.

4.4. Qualitative Description of the Relation Between Bond Lengths and Charges

The changes of the lengths of P-O bonds caused by the affects of the modifier cation were explained [3] using the mechanism of structural variability given by Gutmann [48]. A bond is elongated when electron charge is shifted along the bond from the more electropositive, e. g. P, to the more electronegative atom, e. g. O, and vice versa. This shift is rather a deformation of the electron distribution and not a real electron transfer. The countercharge of a less electronegative modifier atom is completely deposited on the neighboring O_T's which are produced by the rupture of P-O-P links. The cations of strong electric field strength fix this charge on the adjacent O_T's. Otherwise, this negative charge is somewhat shifted to other atomic sites, which has the consequences for the P-O_T and P-O_B bond lengths observed. The P-O_T bond is shortened and the P-O_B bond is elongated. A similar explanation was given by Uchino and Ogata on the basis of ab initio MO calculations of modified silicate glasses [49]. If even O_B's are used in the coordination of the cations, such as in KPO_3 glass, the affects are strengthened.

More electronegative modifier atoms such as Zn or Pb transfer their valence electrons only partially to adjacent O_T sites. With regard to the effects on the P-O bond lengths, this is comparable with the case of cations of strong electric field strength. This behavior may explain the little effects of changes of the P-O bond lengths observed for the glass with the Pb^{2+} cations which is found between those with the Al^{3+} and La^{3+} cations (Chapter 4.3).

The effects of charge transfer are likewise clear in metaphosphate glasses where all the PO_4 tetrahedra have similar environments. In ultra- and polyphosphate glasses two or more differently linked PO_4 units

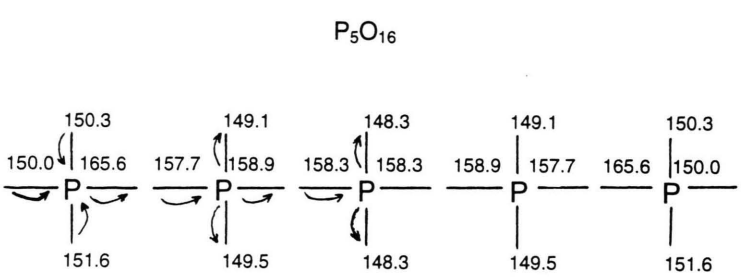

Fig. 9. Model of a P_5O_{16} chain taken from the $Mg_2Na_3P_5O_{16}$ crystal [31]. The bond lengths are given in pm. The small arrows indicate the shift of electron charge along the bonds if compared with the situation in balanced Q^2-Q^2 or Q^1-Q^1 links.

co-exist. As indicated in Fig. 1, the various Q^n units carry different formal charges. As to optimizing the charge compensation of the $Me^{\nu+}$ sites, the electron charge is equalized on all the O_T sites which surround the modifier cations. In this process the O_T atoms of Q^3 units are involved, as well [50]. Thus, electron charge is transfered from Q^n to Q^{n+1} units, which is equivalent with a transfer of π-bonding in opposite direction. In Fig. 5 of [4] this mechanism was illustrated for a Q^3-Q^2 link with the bond lengths taken from the related ZnP_4O_{11} crystal [24]. All the P-O_T bonds tend to equalize while in the P-O-P bridge the difference between both P-O_B distances is increased. These findings agree with the observations made concerning the peak widths of the P-O distances (Chapter 4.2). An example of a polyphosphate is presented in Figure 9. The P-O bond distances in the chains of the crystal $Mg_2Na_3P_5O_{16}$ [31] formed of five PO_4 units obey Gutmann's rule [48] with an electron shift from the O_T atoms of the outer Q^1 to the O_T sites of the Q^2 groups. Consequently, the P-O_B distance of the end group is larger than that in a P_2O_7 diphosphate group (cf. Table 3) because charge is not shifted in the balanced Q^1-Q^1 linkage of the P_2O_7 group. In the chain (Fig. 9) the shortest P-O_B bonds of Q^2 groups are formed in the links with the Q^1 groups. Finally, it is remembered that the conception of the rupture of a P-O-P link and of the subsequent shifts of electron charges accompanied by changes of the lengths of P-O bonds gives a rather formal description of the process of the addition of the modifier cations and the formation of their environmental order.

Only the general trend of the elongation of the P-O_T bond was explained by the bond order conception given in Chapt. 4.1, but not the exact increase. The remaining differences and all the other details of the P-O_T and P-O_B distances result from shifts of electron charges. Surprisingly, in the mean all the changes of the lengths of P-O bonds compensate each other, which leads to a constant mean P-O distance. Deviations from the bond order model were also detected by ^{31}P NMR and Raman spectroscopy of Na and Li ultraphosphate glasses [11, 19]. According to the shift observed for the ν(P=O) band complex, the P-O_T bond of the Q^3 unit is weakened and thus its π-bonding is delocalized [19].

The affects of the fifth valence electron of the phosphorus atom which shortens all the terminal P-O bonds makes phosphate glasses interesting for diffraction studies of high resolution power. Since all the changes of bond lengths compensate each other, a knowledge about the mean P-O distances would not allow to study the related effects. Neutron diffraction studies of similar resolution power in real space performed on other glassy systems, e. g. on silicate glasses, are not successful for use in analogous considerations. A split Si-O peak formed of Si-O_T and Si-O_B distances is not observed [51].

The tendency for the compensation of charges which formally differ for the Q^3 and Q^2 groups of the ultraphosphate glasses may lead to the preference of Q^3-Q^2 linkages [4]. Formally, the countercharge of the modifier cations is deposited on the Q^2 groups. Since the Q^3 units are substantially involved in the environments of the $Me^{\nu+}$ cations [4, 50], linkages between unlike groups should be prefered such as it is found in the related crystal structures [24 - 26]. But in quantitative examinations of the pattern of a 2D ^{31}P MAS NMR experiment of Li ultraphosphate glasses the groups were found to be linked randomly [44].

Analogous considerations of prefered Q^2-Q^1 links are also possible for polyphosphate glasses where the peak widths of the P-O distances (Fig. 6) indicate the shifts of electron charges, as well. A good compensation of charges would be realized in case of the formation of chains of approximately equal lengths. The chain length distributions have been studied for glasses of different modifier cations using high-performance liquid chromatography [52]. The observations indicate an affect of the field strength of the cations. Narrow distributions of the chain lengths result if much of the charge of the valence electrons

of the modifier cations is transfered to the anionic phosphate chains, thus, for alkali cations.

4.5. *The Deformation of PO_4 Tetrahedra Differently Linked*

The peak of the O-O distances at 252 pm in the $T(r)$ function of vitreous P_2O_5 which is shown in [5] indicates the existence of two different lengths of tetrahedral edges. The longer of both distances is attributable to the O_T-O_B edges, whereas the shorter lengths are O_B-O_B edges. This was concluded from a comparison with the PO_4 tetrahedra known from related crystal structures. In case of all the other modified phosphate glasses only a single peak of O-O distances is observed [2 - 4, 6, this work]. The origin of this behavior becomes clear when the O-P-O angles of the four possible PO_4 groups (cf. Fig. 1) are analysed. The O-O distances are strongly affected by the O-P-O angles, more than by the different lengths of the P-O_T and P-O_B bonds. An analysis of the angles is given for four crystals whose structures are formed of only one of the Q^n species. The result is shown in Table 5, where all the angles are related with the concerning edges. The largest angles are formed for edges where O_T atoms are involved, the smallest angles for edges with only O_B atoms. Obviously, the additional negative charge of the π(d-p) fraction of the P-O_T bond does not only shorten the P-O_T distance but it also increases the adjacent O_T-P-O angles.

With the increasing delocalization of π-bonding from the Q^3 up to the Q^0 unit the variation of the six O-P-O angles and the large asymmetry of the PO_4 unit diminishes. Finally, the Q^0 unit is formed as a regular tetrahedron. Presumably, the strong deviations of the Q^3 units from regularity force their change into Q^2 units if modifier oxide is added. A first stabilization is reached if the O_T site of the Q^3 unit can coordinate a modifier cation.

Table 5. The six internal angles O_i-P-O_j of the different PO_4 tetrahedra in four selected crystals which represent the four different Q^n units possible in phosphate structures. i and j stand for T and B which denote the terminal and bridging oxygen atoms, respectively. The angles are given in degree.

Crystalline compound	Six O-P-O angles in the Q^n units of different n					
	1	2	3	4	5	6
o-P_2O_5 (form II)	T-B	T-B	T-B	B-B	B-B	B-B
Q^3	119.8	115.8	115.4	102.3	102.2	99.4
$NaPO_3$ Kurrol A	T-T	T-B	T-B	T-B	T-B	B-B
Q^2	117.1	110.9	110.5	110.4	107.4	99.0
	118.2	110.8	109.8	109.6	108.2	99.2
$Na_4P_2O_7$	T-T	T-T	T-T	T-B	T-B	T-B
Q^1	113.9	112.6	111.6	108.7	106.6	102.5
	113.5	113.2	113.1	107.3	106.3	102.4
Na_3PO_4	T-T	T-T	T-T	T-T	T-T	T-T
Q^0	110.7	110.1	109.9	109.9	109.5	106.7

5. *Conclusions*

In a compositional range, beginning from vitreous P_2O_5 up to pyrophosphate glasses, the behavior of the two P-O distances and of the corresponding peak widths found in phosphate glasses could be studied successfully by neutron diffraction of high resolution power in real space ($Q_{max} \cong 500\,nm^{-1}$). The behavior observed agrees well with that found in the structures of the related crystals and mostly with that resulting from ab initio MO calculations. The elongation of the terminal P-O bonds is mainly attributable to the decrease of their bond order according the delocalization of the fraction of π-bonding on more and more terminal P-O bonds in the progress of the network rupture due to modifier additions. This model implies a constant mean of all the P-O bonds, which is actually observed. Small differences from the simple conception of bond order are explained in terms of shifts of electron charge along the P-O bonds due to the depletion of the valence electrons from the modifier cations to the phosphate network. These effects change the ionicity and, thus, the lengths of the P-O bonds. P-O_T bonds are shortened and P-O_B bonds are elongated. Clear indications for the shifts of electron density are the small widths of the distance peaks of the terminal P-O bonds and the increased widths of the distance peaks of the bridging P-O bonds in glasses where differently linked PO_4 units co-exist. The lengths of the P-O bonds show also variations due to different species of the modifier cation.

Acknowledgements

Financial support of Bundesministerium für Bildung und Forschung (Grant 03-KR5ROK-9) is gratefully acknowledged.

[1] K. Suzuki and M. Ueno, J. Physique, Paris **46,** C8-261 (1985).
[2] U. Hoppe, G. Walter, D. Stachel, and A. C. Hannon, Z. Naturforsch. **50a,** 684 (1995).
[3] U. Hoppe, G. Walter, D. Stachel, and A. C. Hannon, Z. Naturforsch. **51a,** 179 (1996).
[4] U. Hoppe, G. Walter, D. Stachel, A. Barz, and A. C. Hannon, Z. Naturforsch. **52a,** 259 (1997).
[5] U. Hoppe, G. Walter, A. Barz, D. Stachel, and A. C. Hannon, J. Phys.: Condens. Matter **10,** 261 (1998).
[6] U. Hoppe, R. Kranold, D. Stachel, A. Barz, and A. C. Hannon, J. Non-Cryst. Solids **232-234,** 44 (1998).
[7] S. W. Martin, Eur. J. Solid State Inorg. Chem. **29,** 163 (1991).
[8] R. Gresch, W. Müller-Warmuth, and H. Dutz, J. Non-Cryst. Solids **34,** 127 (1979).
[9] E. C. Onyiriuka, J. Non-Cryst. Solids **163,** 268 (1993).
[10] R. K. Brow, J. Non-Cryst. Solids **194,** 267 (1996).
[11] R. K. Brow, D. R. Tallant, J. J. Hudgens, S. W. Martin, and A. D. Irwin, J. Non-Cryst. Solids **177,** 221 (1994).
[12] P. Losso, B. Schnabel, C. Jäger, U. Sternberg, D. Stachel, and D. O. Smith, J. Non-Cryst. Solids **143,** 265 (1992).
[13] A. Lai, A. Musinu, G. Piccaluga, and S. Puligheddu, Phys. Chem. Glasses **38,** 173 (1997).
[14] R. K. Brow, D. R. Tallant, S. T. Myers, and C. C. Phifer, J. Non-Cryst. Solids **191,** 45 (1995).
[15] J. J. Hudgens and S. W. Martin, J. Amer. Ceram. Soc. **76,** 1691 (1993).
[16] A. Barz, K. Meyer, and D. Stachel, Glastech. Ber. Glass Sci. Technol. **68 C1,** 79 (1995).
[17] K. Meyer, J. Non-Cryst. Solids **209,** 227 (1997).
[18] K. Meyer, Phys. Chem. Glasses **39,** 108 (1998).
[19] J. J. Hudgens, R. K. Brow, D. R. Tallant, and S. W. Martin, J. Non-Cryst. Solids **223,** 21 (1998).
[20] C. Dayanand, G. Bhikshamaiah, V. Jaya Tyagaraju, M. Salagram, and A. S. R. Krishna Murthy, J. Mater. Sci. **31,** 1945 (1996).
[21] J. R. Van Wazer, in Phosphorus and its Compounds, Vol. 1, Interscience, New York 1958.
[22] B. C. Sales, J. U. Otaigbe, G. H. Beall, L. A. Boatner, and J. O. Ramey, J. Non-Cryst. Solids **226,** 287 (1998).
[23] El H. Arbib, B. Elouadi, J. P. Chaminade, and J. Darriet, J. Solid State Chem, **127,** 350 (1996).
[24] C. Bäz-Dölle, D. Stachel, I. Svoboda, and H. Fuess, Z. Kristallogr. **203,** 282 (1993).
[25] K.R. Albrund, R. Attig, J. Feener, J. P. Jeser, and D. Mootz, Mater. Res. Bull. **9,** 129 (1974).
[26] D. Stachel, H. Paulus, I. Svoboda, and H. Fuess, Z. Kristallogr. **202,** 117 (1992).
[27] H. van der Meer, Acta Crystallogr. **B32,** 2423 (1976).
[28] J. Matuszewski, J. Kropiwnicka, and T. Znamierowska, J. Solid State Chem. **75,** 285 (1988).
[29] A. McAdam, K. H. Jost, and B. Beagley, Acta Crystallogr. **B24,** 1621 (1968).
[30] K. H. Jost and H. J. Schulze, Acta Crystallogr. **B25,** 1110 (1969).
[31] Y. I. Smolin, Y. F. Shepelev, A. I. Domanski, and J. Majling, Kristallografiya **23,** 1264 (1978).
[32] M. T. Averbuch-Pouchot and A. Durif, Acta Crystallogr. **C43,** 631 (1987).
[33] D. W. J. Cruickshank, Acta Crystallogr. **17,** 674 (1964).
[34] D. F. Mullica, H. O. Perkins, D. A. Grossie, L. A. Boatner, and B. C. Sales, J. Solid State Chem. **62,** 371 (1986).
[35] K. Y. Leung and C. Calvo, Canad. J. Chem. **50,** 2519 (1972).
[36] E. Lissel, M. Jansen, E. Jansen, and G. Will, Z. Kristallogr. **192,** 233 (1990).
[37] A. C. Hannon, W. S. Howells, and A. K. Soper, in Neutron Scattering Data Analysis (Inst. Phys. Conf. Ser. 107), ed. M. W. Johnson, Institute of Physics Publishing, Bristol 1990, p. 193 ff.
[38] R. L. Mozzi and B. E. Warren, J. Appl. Crystallogr. **2,** 164 (1969).
[39] A. C. Wright and A. J. Leadbetter, Phys. Chem. Glasses **17,** 122 (1976).
[40] D. Marquardt, SIAM J. Appl. Math. **11,** 431 (1963).
[41] T. Uchino and Y. Ogata, J. Non-Cryst. Solids **181**, 175 (1995).
[42] A. C. Wright, C. A. Yarker, P. A. V. Johnson, and R. N. Sinclair, J. Non-Cryst. Solids **76,** 333 (1985).
[43] C. Jäger, M. Feike, R. Born, and H. W. Spiess, J. Non-Cryst. Solids **180,** 91 (1994).
[44] T. M. Alam and R. K. Brow, J. Non-Cryst. Solids **223,** 1 (1998).
[45] A. Musinu, G. Paschina, G. Piccaluga, and G. Pinna, J. Non-Cryst. Solids **177,** 97 (1994).
[46] N. J. Kreidl, in Glass: Science and Technology, eds. D. R. Uhlmann and N. J. Kreidl, Academic Press, New York 1983, p. 191 ff.
[47] T. Uchino and Y. Ogata, J. Non-Cryst. Solids **191,** 56 (1995).
[48] V. Gutmann, in The Donor - Acceptor Approach to Molecular Interactions, Plenum Press, New York 1978, pp. 4-16.
[49] T. Uchino, T. Sakka, Y. Ogata, and M. Iwasaki, J. Phys. Chem. **96,** 2455 (1992).
[50] U. Hoppe, J. Non-Cryst. Solids **195,** 138 (1996).
[51] A. C. Hannon, B. Vessal, and J. M. Parker, J. Non-Cryst. Solids **150,** 97 (1992).
[52] B. C. Sales, L. A. Boatner, and J. O. Ramey, J. Non-Cryst. Solids **232-234,** 107 (1998).